

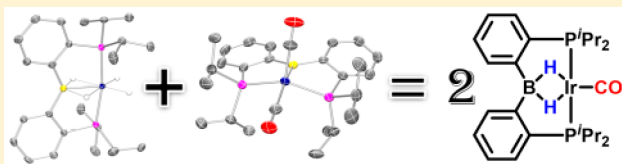
Synthesis and Characterization of PBP Pincer Iridium Complexes and Their Application in Alkane Transfer Dehydrogenation

Wei-Chun Shih and Oleg V. Ozerov*

Department of Chemistry, Texas A&M University, 3255 TAMU, College Station, Texas 77842, United States

S Supporting Information

ABSTRACT: This work reports on the synthesis of several new complexes of Ir supported by a diarylboryl/bis(phosphine) PBP pincer ligand. The previously reported complexes (PBP)Ir(Ph)(Cl) (1) and (PBP)Ir(H)(Cl) (2) were converted to the new complexes (PBP)IrH₄ (3) and (PBP)Ir(Ph)(H) (4). Complexes 3 and 4 serve similarly as precatalysts for transfer dehydrogenation of cyclooctane. The turnover numbers achieved were relatively modest but were increased (to 220 at 200 °C) when 1-hexene was used as a sacrificial hydrogen acceptor vs *tert*-butylethylene. The dicarbonyl complex (PBP)Ir(CO)₂ (6) was also synthesized, by the reaction of CO with either 3 or 4. Intermediates (PB^{Ph}P)Ir(H)(CO)₂ (5) and (PBP)IrH₂(CO) (7) were observed in these reactions. Complex 7 could be obtained in pure form by comproportionation of 3 and 6. Solid-state structures of 3 and 6 were determined by X-ray crystallography.



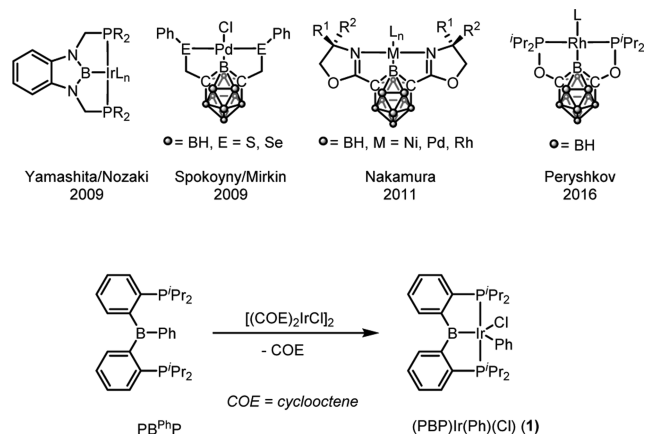
INTRODUCTION

Pincer ligands are a particularly advantageous class of ancillary ligands in transition-metal chemistry that have allowed for the pursuit of well-defined fundamental reactivity as well as given rise to impressive catalytic applications.¹ Alkane dehydrogenation and the associated catalytic transformations of hydrocarbons are among the most impressive accomplishments for pincers in catalysis.^{2–4}

Although diverse designs abound, the most common construction of a pincer ligand combines flanking phosphine side arms with a different central donor. Among these central donors, boryls have been among the latest to be introduced. Boryls are particularly interesting because they are arguably the most donating and the most trans influencing among donor ligands that can be incorporated into polydentate ligands. The first boryl/bis(phosphine) PBP* pincer ligand was reported by Nozaki and Yamashita in 2009 (Chart 1).⁵ In the following years, several groups accessed boryl-centered pincer ligands where the boryl donor is incorporated into an *m*-carborane cage (Chart 1).⁶ Yamashita later reported a study testing the utility of PBP* complexes of Ir in alkane dehydrogenation, with modest success.⁷ Yamashita's PBP* ligand has also been used by other groups.⁸

In a previous publication,⁹ we showed how insertion of an Ir center into a B–Ph bond of a PB^{Ph}P precursor¹⁰ provides access to the new boryl/bis(phosphine) complex (PBP)Ir(Ph)(Cl) (1; Chart 1). Palladium complexes of this PBP pincer were recently reported by Tauchert et al.¹¹ We reported⁹ that complex 1 can be converted to the hydrido/chloride 2 via intermediacy of 2-H₂ in an overall hydrogenolysis reaction (Scheme 1). In order to evaluate the potential of the (PBP)Ir system in alkane dehydrogenation, we sought to prepare a (PBP)Ir polyhydride derivative. In addition, we envisaged synthesizing a carbonyl derivative for the purpose of comparing

Chart 1. Previously Reported Pincer Complexes with a Central Boryl Donor (Top) and Synthesis of Complex 1 by Insertion into a B–Ph Bond (Bottom)



the apparent donor ability of the PBP ligand toward Ir in comparison with other pincer ligands. Herein we report the results of these pursuits.

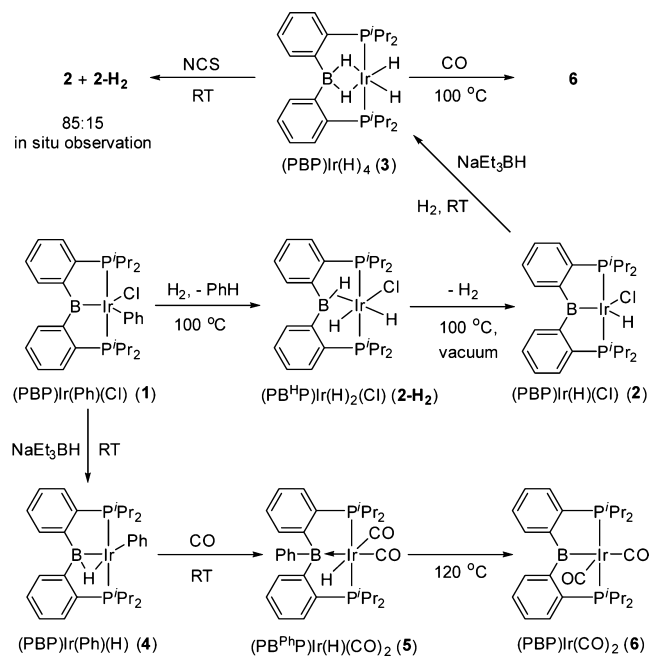
RESULTS AND DISCUSSION

Synthesis and Characterization of PBP-Type Pincer Iridium Complexes. Stirring 2 and sodium triethylborohydride in toluene or C₆D₆ at room temperature followed by placing the reaction mixture under 1 atm of H₂ afforded a pale yellow solution of (PBP)IrH₄ (3), from which a 64% isolated

Special Issue: Hydrocarbon Chemistry: Activation and Beyond

Received: September 28, 2016

Scheme 1. Synthesis and Reactivity of (PBP)Ir Complexes



yield was obtained upon workup (Scheme 1).¹² Treatment of solutions of **3** with 1.0 equiv of *N*-chlorosuccinimide (NCS) at room temperature was found to convert **3** back to **2**. The in situ mixture contained $(\text{PB}^{\text{H}}\text{P})\text{Ir}(\text{H})_2(\text{Cl})$ (**2-H}_2**) and $(\text{PBP})\text{Ir}(\text{H})(\text{Cl})$ (**2**) in a 15:85 ratio, and the removal of volatiles at 100°C under vacuum fully converted the mixture into **2**. Complex **3** displayed C_{2v} symmetry in its ^1H NMR spectrum, with two different hydride resonances apparent: a broad signal at $\delta -6.82$ ppm and a triplet at $\delta -13.47$ ppm (t, $J_{\text{H-P}} = 12.7$ Hz). We ascribe these resonances to the pair of bridging and terminal hydrides, respectively. A similar picture was observed in the hydride region by Lin and Peters for $(\text{PBP}^*)\text{CoH}_4$,^{8a} albeit only at -90°C and under an H_2 atmosphere ($\text{PBP}^* = \text{Yamashita's PBP ligand}$).

An X-ray diffraction study (Figure 1) of **3** permitted identification of the two bridging hydride ligands H1 and H2 and the two terminal hydride ligands H7 and H8, located via the Fourier difference map. Radius, Braunschweig, et al. discussed the limiting structural motifs for complexes of $[\text{R}_2\text{BH}_2]^-$ fragments with transition metals (Chart 2).¹³ They argued that a more Lewis acidic boron center favors structural type A (κ^2 -dihydroborate) over B (σ -B-H complex of a metal hydride), whereas a more electron-rich metal would favor the higher valence type C (boryl/dihydride). It should be noted that type B may correspond to two degenerate forms (B and B'), which may average out to a more symmetric structure: for example, by NMR spectroscopy. These issues have been explored in detail by Sabo-Etienne and co-workers in Ru chemistry.¹⁴ In addition, A and C can be viewed as limiting structures at either end of a possible continuum of intermediate structures. In this vein, Yamashita et al. ascribed type D to the structures of $(\text{PBP}^*)(\mu\text{-H})_2\text{RuX}$ (where $\text{X} = \text{BH}_4$,¹⁵ OAc ¹⁶). These compounds possessed a Ru-B bond distance comparable to that of unambiguous 2c-2e Ru-B_{boryl} bonds yet clearly contained bridging hydrides. D can be viewed as either incomplete insertion of the metal into the pair of B-H bonds in type A or as a variation of C that retains B...H contacts.

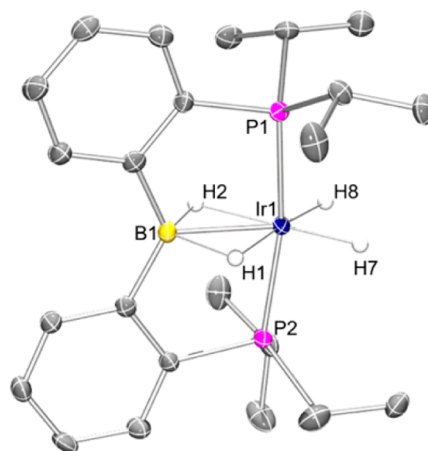
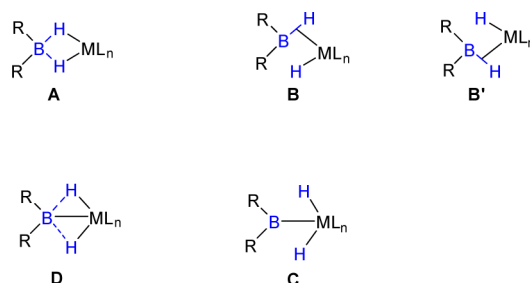


Figure 1. POV-Ray rendition of the ORTEP drawing (50% thermal ellipsoids) of **3** showing selected atom labeling. Hydrogen atoms are omitted, except for the hydrogens on Ir, for clarity. Selected bond distances (Å) and angles (deg): Ir1-B1, 2.159(3); Ir1-H1, 1.64(3); Ir1-H2, 1.71(3); Ir1-H7, 1.57(3); Ir1-H8, 1.50(3); B1-H1, 1.48(3); B1-H2, 1.34(3); Ir1-P1, 2.2840(7); Ir1-P2, 2.2804(7); B1-Ir1-H1, 43.3(10); B1-Ir1-H2, 38.3(10); B1-Ir1-H7, 138.6(11); B1-Ir1-H8, 139.9(10); H1-Ir1-H8, 176.0(14); H2-Ir1-H7, 176.0(13); H1-B1-H2, 101.5(17); H7-Ir1-H8, 81.5(15).

Chart 2. Different Structural Types for Interaction of R_2BH_2 with a Transition Metal, As Presented by Radius and Braunschweig (A-C), and Yamashita's Assignment of the Intermediate Structure D



The $\text{Ir}\cdots\text{B}$ bond distance in **3** (2.159(3) Å) is shorter than the $\text{Ir}\cdots\text{B}_{\text{borate}}$ bond distances (2.19–2.28 Å) in the dihydrido borate iridium complexes. It is slightly longer than the Ir-B distances in **2-H}_2** (2.135–2.137 Å) possessing a σ -B-H coordination mode.^{7,9} Although this distance is ca. 0.15 Å longer than the 2c-2e Ir-B bonds in **1** and **2**, it is only ca. 0.02 Å longer than the 2c-2e Ir-B distance in **6** (vide infra). The $^{11}\text{B}\{^1\text{H}\}$ NMR chemical shift observed for **3** (45.6 ppm; Table 1) is decidedly upfield of that for the unambiguous boryl species but also clearly not upfield enough to fall in the region of sp^3 -hybridized B. On the basis of these observations, it seems reasonable to suggest that complex **3** lies somewhere along the continuum between A and C, and probably closer to type A. The fact that the solid-state structure is symmetric with respect

Table 1. Chemical Shifts in $^{11}\text{B}\{^1\text{H}\}$ NMR and $^{31}\text{P}\{^1\text{H}\}$ NMR Spectra of Ir Complexes (in ppm)

	1	2	2-H}_2	3	4	5	6	7
^{11}B	75.9	72.6	53.7	45.6	53.1	5.7	99.4	42.4
^{31}P	44.9	61.9	53.5	65.4	56.8	51.7	61.0	66.2

to the B–Ir vector argues against **B** as the ground state, at least in the solid.

Another potential transfer dehydrogenation precatalyst (PBP)Ir(Ph)(H) (**4**) was also successfully synthesized (Scheme 1). Stirring **1** and sodium triethylborohydride in toluene or C₆D₆ at room temperature resulted in an immediate formation of a dark red solution. Solution multinuclear NMR analysis demonstrated the near-quantitative formation of complex **4**. Relative to **1** (75.9 ppm) or **2** (72.6 ppm), the ¹¹B NMR resonance of **4** (53.1 ppm) is shifted considerably upfield, and the hydride resonance (δ –11.51 ppm) is broad, which suggests a degree of interaction between B and H in **4** that is not present in **2**. This interaction is likely also responsible for the thermal stability of **4** with respect to reductive elimination of benzene, as it lowers the energy of **4** as a benzene addition product to (PBP)Ir. Without the auxiliary B–H interaction, elimination of benzene from **4** would be expected to be quite facile.¹⁷

Exposure of a solution of **4** to 1 atm of CO led to the formation of a pale yellow solution of (PB^{Ph}P)Ir(H)(CO)₂ (**5**) after a few minutes (Scheme 1). The presence of two carbonyl ligands was evident from the two downfield ¹³C NMR resonances (179.0 and 168.5 ppm) as well as two bands in the IR spectrum (ν_{CO} 2015 and 1978 cm^{–1}). The ¹¹B NMR spectrum showed one upfield resonance at 5.7 ppm, consistent with an sp³-hybridized boron. One triplet peak at –10.66 ppm (t , $J_{\text{H-P}} = 15.0$ Hz, Ir–H) in the ¹H NMR spectrum showed no broadening from interaction with boron, consistent with a terminal Ir hydride. These observations suggest the structure of **5** as depicted in Scheme 1, with the triarylborane moiety acting as a Z-type ligand. Triarylboranes have been at the center of the development of new appreciation for Z-type ligands over the past decade or so.^{18–21} The formation of **5** can be viewed as CO-induced reductive elimination of a B–C bond from **4**.

Thermolysis of complex **4** at 120 °C under a CO atmosphere led to a gradual change in the color of the solution to dark-red, corresponding to the formation of the new complex (PBP)Ir(CO)₂ (**6**). Conversion of the intermediately formed **5** into **6** requires loss of benzene. While we have not ascertained the mechanism by which this happens, a likely scenario involves migration of Ph to Ir with loss of CO, followed by C–H reductive elimination of benzene and recoordination of CO.

The downfield ¹¹B NMR chemical shift (99.4 ppm; Table 1) confirmed the presence of an sp²-hybridized boryl central donor in **6**. Complex **6** displayed C_{2v} symmetry in solution on the NMR time scale at room temperature: a singlet resonance at 61.0 ppm in the ³¹P{¹H} NMR spectrum, one methine resonance and two methyl resonances from the isopropyl groups in the ¹H NMR spectrum, and one CO resonance in the ¹³C{¹H} NMR spectrum. However, the solid-state IR spectrum revealed two CO stretching bands at 1960 and 1913 cm^{–1}. The presence of two coordinated carbonyls was confirmed in the course of an X-ray diffraction study on a single crystal of **6** (Figure 2). The geometry about Ir in **6** is distorted five-coordinate and is closer to square pyramidal than to trigonal bipyramidal (the τ parameter²² is 0.33). The solid-state structure is approximately C_s symmetric. The C_{2v} symmetry on the NMR time scale in solution suggests that rapid interconversion between the degenerate, less symmetric ground state forms takes place rapidly. The sum of angles about the boron center was found to be 360°, consistent with a trigonal-planar, sp²-hybridized boryl. However, the Ir–B distance (2.137 Å) was decidedly longer than typical PBP-type Ir–B_{boryl}

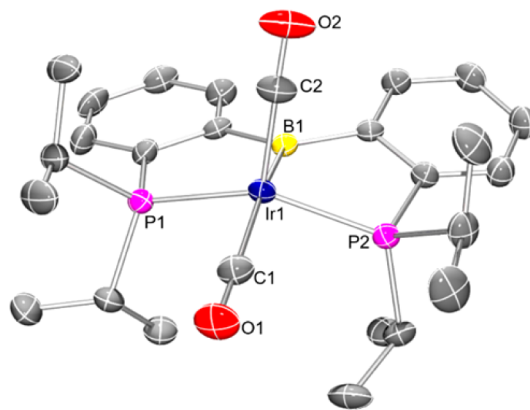


Figure 2. POV-Ray rendition of the ORTEP drawing (50% thermal ellipsoids) of **6** showing selected atom labeling. Hydrogen atoms are omitted for clarity. Selected bond distances (Å) and angles (deg): Ir1–B1, 2.137(3); Ir1–C1, 1.935(3); Ir1–C2, 1.890(3); C1–O1, 1.144(4); C2–O2, 1.142(4); Ir1–P1, 2.3082(14); Ir1–P2, 2.2985(13); B1–Ir1–C1, 159.32(13); B1–Ir1–C2, 88.42(13); C1–Ir1–C2, 112.26(14); P1–Ir1–P2, 139.45(3); C2–Ir1–P1, 109.97(11); C2–Ir1–P2, 104.32(12).

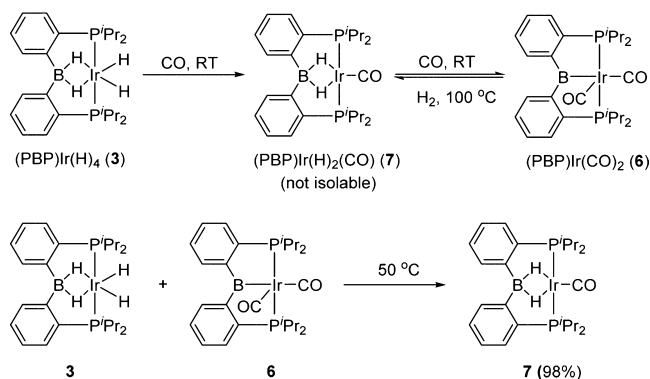
distances (1.97–2.05 Å).^{5,7,9} The origin of this relative elongation in **6** is not clear.

Monovalent Ir complexed by PXP-type pincer ligands typically prefers to bind only a single carbonyl ligand. Although coordination of the second CO is possible, it is typically bound weakly and readily lost upon workup and/or exposure to vacuum.^{23,24} The fact that **6** persists as a dicarbonyl in solution in the absence of a CO atmosphere is thus rather unusual. It is possible that the strongly donating nature of the boryl ligand improves back-bonding to CO ligands, resulting in stronger bonds. On the other hand, it is also reasonable to suggest that the putative square planar monocarbonyl complex may be destabilized by the tenuous placement of the very strongly trans influencing boryl trans to CO.

Complex **6** can also be synthesized by addition of 1 atm of CO to a toluene solution of **3** at 100 °C overnight via loss of 2 equiv of H₂. When **3** was exposed to an atmosphere of CO at room temperature for 1 h, the new intermediate (PBP)Ir(H)₂(CO) (**7**) was observed to constitute 52% of the mixture, along with 22% of **3** and some other unidentifiable products (percentages of total ³¹P NMR intensity given). This reaction mixture gradually evolved into a dark red solution that contained 43% of **6** (³¹P NMR evidence) after 24 h. The reverse reaction was observed during the thermolysis of the C₆D₆ solution of **6** under 1 atm of H₂ at 100 °C overnight, yielding a mixture of **7** and **6** in a ratio of 41 to 47, with the balance being due to two minor unidentified products. Although a pure bulk sample of **7** could not be isolated by the reaction of **3** with CO due to the facile conversion to **6**, it was easily synthesized by comproportionation of **3** and **6** at 50 °C in toluene (Scheme 2). The signal in the ¹¹B{¹H} NMR spectrum and a broad resonance of the bridging hydrides in the ¹H NMR spectrum of **7** (42.4 and –6.26 ppm) are similar to those of compound **3** (45.6 and –6.82 ppm). It can be concluded that the same arguments (vide supra) regarding the nature of the apparent dihydroborate binding to Ir are applicable to **7** as well as **3**.

Transfer Dehydrogenation of COA to COE Catalyzed by (PBP)Ir(H)₄ (3**) and (PBP)Ir(Ph)(H) (**4**).** Complexes **3** and **4** were tested as precatalysts for transfer dehydrogenation of

Scheme 2. Comproportionation of 3 and 6 into 7



cyclooctane (COA) to cyclooctene (COE) with *tert*-butylethylene (TBE) or 1-hexene as the hydrogen acceptor (Table 2). A significant amount of work on related PCP/POCOP-type

Table 2. TONs for Dehydrogenation of COA to COE Catalyzed by $(\text{PBP})\text{Ir}(\text{H})_4$ (3) and $(\text{PBP})\text{Ir}(\text{Ph})(\text{H})$ (4)^a

entry	cat.	R	T (°C)	time (h)	TON
1	3	CMe ₃	100	26	0
2	3	CMe ₃	150	26	30
3	3	CMe ₃	200	0.5	32
4	3	CMe ₃	200	1	34
5	3	CMe ₃	200	2	36
6	3	CMe ₃	200	4	36
7	3	CMe ₃	200	6	36
8	3	CMe ₃	200	26	43
9	3	ⁿ Bu	150	26	78
10	3	ⁿ Bu	200	26	221
11	4	CMe ₃	150	26	38
12	4	CMe ₃	200	15	47
13	4	ⁿ Bu	200	26	158

^aTONs were calculated on the basis of the formation of COE in ¹H NMR with mesitylene (3.59 mmol) as internal standard. Reaction conditions: COA (10.0 mmol), TBE or 1-hexene (10.0 mmol), cat. 3 or 4 (0.01 mmol).

pincer complexes of Ir indicates that intermediacy of the monovalent [(pincer)Ir] fragment is crucial.³ 3 and 4 may be able to access a corresponding transient (PBP)Ir intermediate via reductive elimination of benzene or H₂ or by hydrogenation of the sacrificial olefin. Although there was no conversion at 100 °C (entry 1), a turnover number (TON) of 30 was achieved at 150 °C for 26 h (entry 2). The TONs were slightly increased to 43 upon elevation of the reaction temperature to 200 °C (entry 8), but it was clear that most of the TONs took place early in the reaction (entries 3–7). Utilization of the sterically less imposing 1-hexene instead of TBE as the hydrogen acceptor enhanced the obtained TONs to 78 at 150 °C and 221 at 200 °C (entries 9 and 10).²⁵ Using complex 4 as the precatalyst with TBE or 1-hexene as the hydrogen acceptor gave TONs (entries 11–13) similar to those for use of 3 as the precatalyst. The activities of 3 and 4 as precatalysts for alkane transfer dehydrogenation are modestly higher than those of Yamashita's Ir complexes supported by the PBP* ligand.⁷

However, they fall significantly short of the best Ir examples utilizing pincer ligands of the aryl/bis(phosphine) type.^{3,4}

CONCLUSION

In summary, we report the preparation of new diarylboryl/bis(phosphine) PBP complexes of Ir that can serve as precatalysts for alkane transfer dehydrogenation. The activity displayed by this system was found to be modest. Structural and spectroscopic characterization of a series of PBP complexes enabled analysis of nonclassical BH/Ir interactions.

EXPERIMENTAL SECTION

General Considerations. Unless specified otherwise, all manipulations were performed under an Ar atmosphere using standard Schlenk line or glovebox techniques. Screw-capped culture tubes with PTFE-lined phenolic caps were used to perform catalytic reactions. Toluene, pentane, and isooctane were dried and deoxygenated (by purging) using a solvent purification system (Innovative Technology Pure Solv MD-5 Solvent Purification System) and stored over molecular sieves in an Ar-filled glovebox. C₆D₆ was dried over NaK/Ph₂CO/18-crown-6, distilled or vacuum-transferred, and stored over molecular sieves in an Ar-filled glovebox. Hexamethyldisiloxane, COA, 1-hexene, and TBE were degassed by three freeze–pump–thaw cycles and stored over molecular sieves in an Ar-filled glovebox. (PBP)Ir(Ph)(Cl) (1), (PB^HP)Ir(H)₂(Cl) (2-H₂), and (PBP)Ir(H)(Cl) (2) were prepared via literature procedures.⁹ All other chemicals were used as received from commercial vendors. NMR spectra were recorded on a Varian Inova 400 (¹H NMR, 399.535 MHz; ¹³B NMR, 128.185 MHz; ³¹P NMR, 161.734 MHz) or a Varian Inova 500 (¹H NMR, 499.703 MHz; ¹³C NMR, 125.697 MHz; ³¹P NMR, 202.265 MHz) spectrometer. Chemical shifts are reported in δ (ppm). Coupling constant values in the ¹H NMR spectra should be interpreted with a 0.2 Hz uncertainty. For ¹H and ¹³C NMR spectra, the residual solvent peak was used as an internal reference (¹H NMR, δ 7.16 for C₆D₆; ¹³C NMR, δ 128.06 for C₆D₆). ¹B NMR spectra were referenced externally with BF₃ etherate at δ 0. ³¹P NMR spectra were referenced externally with 85% phosphoric acid at δ 0. Elemental analyses were performed by CALI Laboratories, Inc. (Parsippany, NJ).

(PBP)Ir(H)₄ (3). In a 25 mL Teflon screw-capped round-bottomed flask, NaEt₃BH (500 μL, 0.50 mmol, 1.0 M in toluene) was added to a toluene solution (2 mL) of (PBP)Ir(H)(Cl) (2; 313 mg, 0.50 mmol). The solution was degassed via freeze–pump–thaw, and the flask was refilled with H₂ (1 atm). The reaction mixture was stirred at room temperature for 1 h. During the stirring, the solution gradually changed from dark red to pale yellow. The solution was filtered through Celite, and the volatiles were removed under vacuum. The resulting solid was washed with isooctane, yielding a pale yellow solid (189 mg, 64%). ³¹P{¹H} NMR (202 MHz, C₆D₆): δ 65.4. ¹B NMR (128 MHz, C₆D₆): δ 45.6 (br). ¹H NMR (500 MHz, C₆D₆): δ 8.62 (d, J_{H,H} = 7.5 Hz, 2H, Ar-H), 7.43 (m, 2H, Ar-H), 7.30 (t, J_{H,H} = 7.4 Hz, 2H, Ar-H), 7.15 (m, 2H, Ar-H), 2.18 (m, 4H, CHMe₂), 1.24 (dvt, J_{H,H} ≈ J_{H,P} = 7.3 Hz, 12H, CHMe₂), 0.98 (dvt, J_{H,H} ≈ J_{H,P} = 7.1 Hz, 12H, CHMe₂), −6.82 (br s, 2H, B-H₂-Ir), −13.47 (t, J_{H,P} = 12.7 Hz, 2H, Ir-H₂). ¹³C{¹H} NMR (101 MHz, C₆D₆): δ 162.6 (br s, C-B), 149.3 (vt, J_{P,C} = 22.7 Hz, C-P), 131.5 (vt, J_{P,C} = 7.8 Hz), 130.5 (s), 130.3 (s), 126.2 (vt, J_{P,C} = 3.5 Hz), 26.6 (vt, J_{P,C} = 15.7 Hz, CHMe₂), 20.9 (t, J_{P,C} = 2.8 Hz, CHMe₂), 19.0 (s, CHMe₂). Anal. Calcd for C₂₄H₄₀BIrP₂: C, 48.57; H, 6.79. Found: C, 48.65; H, 6.59. Mp: 190 °C dec.

(PBP)Ir(H)(Ph) (4). In a 50 mL Schlenk flask, NaEt₃BH (1.00 mL, 1.00 mmol, 1.0 M in toluene) was added to a toluene solution (10 mL) of (PBP)Ir(Ph)(Cl) (1; 702 mg, 1.00 mmol). The reaction mixture was stirred at room temperature for 1 h. The solution was filtered through Celite, and the volatiles were removed under vacuum. The resulting solid was washed with hexamethyldisiloxane, yielding an orange solid (567 mg, 93%). ³¹P{¹H} NMR (202 MHz, C₆D₆): δ 56.8. ¹B NMR (128 MHz, C₆D₆): δ 53.1 (br). ¹H NMR (500 MHz, C₆D₆): δ 8.50 (d, J_{H,H} = 7.1 Hz, 2H), 7.43 (d, J_{H,H} = 6.7 Hz, 1H), 7.36 (m, 4H), 7.21 (m, 5H), 6.93 (t, J_{H,H} = 7.0 Hz, 1H), 2.57 (m, 2H, CHMe₂),

2.49 (m, 2H, CHMe₂), 1.18 (dvt, $J_{\text{H,H}} \approx J_{\text{H,P}} = 7.3$ Hz, 6H, CHMe₂), 1.09 (dvt, $J_{\text{H,H}} \approx J_{\text{H,P}} = 7.3$ Hz, 6H, CHMe₂), 0.94 (dvt, $J_{\text{H,H}} \approx J_{\text{H,P}} = 6.7$ Hz, 6H, CHMe₂), 0.84 (dvt, $J_{\text{H,H}} \approx J_{\text{H,P}} = 7.3$ Hz, 6H, CHMe₂), −11.51 (br s, 1H, Ir-H). ¹³C{¹H} NMR (101 MHz, C₆D₆): δ 165.0 (t, $J_{\text{P,C}} = 8.6$ Hz, Ir-C), 161.2 (br s, C-B), 145.3 (vt, $J_{\text{P,C}} = 23.5$ Hz, C-P), 138.1 (s), 130.4 (m), 129.9 (s), 128.6 (s), 126.9 (vt, $J_{\text{P,C}} = 3.2$ Hz), 125.0 (s), 121.5 (s), 25.5 (vt, $J_{\text{P,C}} = 13.6$ Hz, CHMe₂), 23.4 (vt, $J_{\text{P,C}} = 14.5$ Hz, CHMe₂), 20.5 (s, CHMe₂), 19.0 (s, CHMe₂), 18.8 (s, CHMe₂), 17.4 (s, CHMe₂). Anal. Calcd for C₃₀H₄₂BrIrP₂: C, 53.97; H, 6.34. Found: C, 53.68; H, 6.46. Mp: 114 °C dec.

(PBP^{Ph})Ir(H)(CO)₂ (5). In a 25 mL Teflon screw-capped round-bottomed flask, (PBP)Ir(H)(Ph) (4; 67 mg, 0.10 mmol) was dissolved in C₆H₆ (1.0 mL). The solution was degassed twice via freeze–pump–thaw, and the flask was refilled with CO (1 atm). After 10 min, the solution changed from orange to pale yellow. The volatiles were removed under vacuum, and the resulting solid was washed with cold pentane, yielding a pale yellow solid (52 mg, 72%). The purity of isolated samples of **5** was gauged to be >95% by NMR spectroscopy. ³¹P{¹H} NMR (202 MHz, C₆D₆): δ 51.7. ¹¹B NMR (128 MHz, C₆D₆): δ 5.7. ¹H NMR (500 MHz, C₆D₆): δ 7.81 (d, $J_{\text{H,H}} = 7.3$ Hz, 2H), 7.20 (t, $J_{\text{H,H}} = 7.3$ Hz, 2H), 7.16 (m, 2H), 7.12 (m, 2H), 7.03 (t, $J_{\text{H,H}} = 6.7$ Hz, 2H), 6.96 (t, $J_{\text{H,H}} = 7.2$ Hz, 1H), 6.89 (d, $J_{\text{H,H}} = 7.2$ Hz, 2H), 2.37 (m, 2H, CHMe₂), 2.27 (m, 2H, CHMe₂), 1.14 (dvt, $J_{\text{H,H}} \approx J_{\text{H,P}} = 7.3$ Hz, 6H, CHMe₂), 0.99 (m, 12H, CHMe₂), 0.69 (dvt, $J_{\text{H,H}} \approx J_{\text{H,P}} = 7.3$ Hz, 6H, CHMe₂), −10.66 (t, $J_{\text{H,P}} = 15.0$ Hz, 1H, Ir-H). ¹³C{¹H} NMR (101 MHz, C₆D₆): δ 179.0 (s, CO), 174.2 (br, B-C_{Ar}), 168.5 (s, CO), 164.6 (br, B-C_{Ph}), 141.4 (vt, $J_{\text{P,C}} = 30.3$ Hz, C-P), 135.7 (s), 133.8 (vt, $J_{\text{P,C}} = 11.0$ Hz), 129.6 (s), 128.5 (vt, $J_{\text{P,C}} = 3.5$ Hz), 126.1 (s), 124.2 (vt, $J_{\text{P,C}} = 4.2$ Hz), 124.1 (s), 29.7 (vt, $J_{\text{P,C}} = 13.7$ Hz, CHMe₂), 27.9 (vt, $J_{\text{P,C}} = 17.9$ Hz, CHMe₂), 20.2 (s, CHMe₂), 20.1 (s, CHMe₂), 19.5 (s, CHMe₂), 18.6 (s, CHMe₂). IR (KBr), ν_{CO} 2015, 1978 cm^{−1}.

(PBP)Ir(CO)₂ (6). *Method A.* In a 25 mL Teflon screw-capped round-bottomed flask, (PBP)Ir(H)₄ (3; 89 mg, 0.15 mmol) was dissolved in toluene (2 mL). The solution was degassed twice via freeze–pump–thaw, and the flask was refilled with CO (1 atm). The reaction mixture was stirred at 100 °C overnight. During the heating, the color gradually changed from pale yellow to dark red. The volatiles were removed under vacuum, and the resulting solid was washed with cold pentane, yielding a dark red solid (80 mg, 83%).

Method B. In a 25 mL Teflon screw-capped round-bottomed flask, (PBP)Ir(H)(Ph) (4; 134 mg, 0.20 mmol) was dissolved in toluene (2 mL). The solution was degassed twice via freeze–pump–thaw, and the flask was refilled with CO (1 atm). The reaction mixture was stirred at 120 °C for 3 days. The volatiles were removed under vacuum, and the resulting solid was washed with cold pentane, yielding a dark red solid (98 mg, 76%). ³¹P{¹H} NMR (202 MHz, C₆D₆): δ 61.0. ¹¹B NMR (128 MHz, C₆D₆): δ 99.4 (br). ¹H NMR (500 MHz, C₆D₆): δ 8.09 (d, $J_{\text{H,H}} = 7.4$ Hz, 2H), 7.38 (m, 2H), 7.20 (m, 2H), 7.11 (m, 2H), 2.31 (m, 4H, CHMe₂), 1.09 (dvt, $J_{\text{H,H}} \approx J_{\text{H,P}} = 6.9$ Hz, 12H, CHMe₂), 0.90 (dvt, $J_{\text{H,H}} \approx J_{\text{H,P}} = 6.9$ Hz, 12H, CHMe₂). ¹³C{¹H} NMR (126 MHz, C₆D₆): δ 185.6 (s, CO), 163.2 (br s, C-B), 152.2 (vt, $J_{\text{P,C}} = 25.2$ Hz, C-P), 130.4 (vt, $J_{\text{P,C}} = 11.1$ Hz), 130.1 (s), 129.4 (s), 128.6 (s), 28.8 (vt, $J_{\text{P,C}} = 14.3$ Hz, CHMe₂), 19.74 (vt, $J_{\text{P,C}} = 2.4$ Hz, CHMe₂), 18.43 (s, CHMe₂). IR (KBr), ν_{CO} 1960, 1913 cm^{−1}. Anal. Calcd for C₂₆H₃₆BrIrO₂P₂: C, 48.38; H, 5.62. Found: C, 48.76; H, 5.68.

(PBP)Ir(H)₂(CO) (7). In a 25 mL Teflon screw-capped round-bottomed flask, (PBP)Ir(H)₄ (3; 237 mg, 0.40 mmol) and (PBP)Ir(CO)₂ (6; 284 mg, 0.44 mmol) were dissolved in toluene (10 mL). The reaction mixture was stirred at 50 °C overnight. During the heating, the mixture gradually changed from dark red to orange. After the mixture was cooled to room temperature, the volatiles were removed under vacuum, and the resulting solid was redissolved in toluene, layered with pentane, and placed in a −35 °C freezer, yielding orange crystals (486 mg, 98%). The purity of isolated samples of **7** was gauged to be >95% by NMR spectroscopy. ³¹P{¹H} NMR (202 MHz, C₆D₆): δ 66.2. ¹¹B NMR (128 MHz, C₆D₆): δ 42.4 (br). ¹H NMR (500 MHz, C₆D₆): δ 8.38 (d, $J_{\text{H,H}} = 7.5$ Hz, 2H), 7.31 (m, 2H), 7.27 (m, 2H), 7.09 (td, $J_{\text{H,H}} = 7.4$, $J_{\text{H,H}} = 1.2$ Hz, 2H), 2.22 (m, 4H, CHMe₂),

1.24 (dvt, $J_{\text{H,H}} \approx J_{\text{H,P}} = 6.9$ Hz, 12H, CHMe₂), 0.89 (dvt, $J_{\text{H,H}} \approx J_{\text{H,P}} = 7.0$ Hz, 12H, CHMe₂), −6.26 (br s, 2H, Ir-H). ¹³C{¹H} NMR (126 MHz, C₆D₆): δ 187.0 (s, CO), 162.4 (br s, C-B), 146.9 (vt, $J_{\text{P,C}} = 25.8$ Hz, C-P), 132.0 (vt, $J_{\text{P,C}} = 8.6$ Hz), 130.3 (s), 130.0 (vt, $J_{\text{P,C}} = 2.3$ Hz), 126.1 (vt, $J_{\text{P,C}} = 3.9$ Hz), 28.1 (vt, $J_{\text{P,C}} = 15.7$ Hz, CHMe₂), 20.3 (vt, $J_{\text{P,C}} = 1.8$ Hz, CHMe₂), 18.9 (s, CHMe₂).

General Procedure of Transfer Dehydrogenation of COA using Complex 3. In a screw-capped culture tube, complex **3** (5.9 mg, 0.01 mmol) was dissolved in a solution of COA (1.35 mL, 10.0 mmol) and a hydrogen acceptor (1.29 mL for TBE or 1.25 mL for 1-hexene, 10.0 mmol). The tube was sealed, and the reaction mixture was heated in a preheated oil bath at a suitable temperature for the required time (Table 2, entries 1–10). After the tube was cooled to room temperature, mesitylene (0.50 mL, 3.59 mmol) was added as internal standard and the TON was calculated on the basis of the formation of COE in the ¹H NMR spectrum.

General Procedure of Transfer Dehydrogenation of COA using Complex 4. In a screw-capped culture tube, complex **4** (6.7 mg for **4**, 0.01 mmol) was dissolved in a solution of COA (1.35 mL, 10.0 mmol) and a hydrogen acceptor (1.29 mL for TBE or 1.25 mL for 1-hexene, 10.0 mmol). The tube was sealed, and the reaction mixture was heated in a preheated oil bath at a suitable temperature for the required time (Table 2, entries 11–13). After the tube was cooled to room temperature, mesitylene (0.50 mL, 3.59 mmol) was added as internal standard and the TON was calculated on the basis of the formation of COE in the ¹H NMR spectrum.

X-ray Data Collection, Solution, and Refinement for (PBP)Ir(H)₄ (3). A colorless, multifaceted block of suitable size (0.26 × 0.09 × 0.04 mm) was selected from a representative sample of crystals of the same habit using an optical microscope and mounted onto a nylon loop. Low-temperature (110 K) X-ray data were obtained on a Bruker APEXII CCD-based diffractometer (Mo sealed X-ray tube, $K\alpha$ 0.71073 Å). All diffractometer manipulations, including data collection, integration, and scaling, were carried out using the Bruker APEXII software.²⁶ An absorption correction was applied using SADABS.²⁷ The space group was determined on the basis of systematic absences and intensity statistics, and the structure was solved by direct methods and refined by full-matrix least squares on F^2 . The structure was solved in the monoclinic $P2_1/c$ space group using XS²⁸ (incorporated in SHELXL). All non-hydrogen atoms were refined with anisotropic thermal parameters. All hydrogen atoms were placed in idealized positions and refined using a riding model, with the exception of the hydrogen bound to iridium, which was located from the difference map. The structure was refined (weighted least-squares refinement on F^2), and the final least-squares refinement converged. No additional symmetry was found using ADDSYM incorporated in the PLATON program.²⁹

X-ray Data Collection, Solution, and Refinement for (PBP)Ir(CO)₂ (6). A red, multifaceted block of suitable size (0.20 × 0.16 × 0.04 mm) was selected from a representative sample of crystals of the same habit using an optical microscope and mounted onto a nylon loop. Low-temperature (150 K) X-ray data were obtained on a Bruker APEXII CCD-based diffractometer (Mo sealed X-ray tube, $K\alpha$ = 0.71073 Å). All diffractometer manipulations, including data collection, integration, and scaling, were carried out using the Bruker APEXII software.²⁶ An absorption correction was applied using SADABS.²⁷ The space group was determined on the basis of systematic absences and intensity statistics, and the structure was solved by direct methods and refined by full-matrix least squares on F^2 . The structure was solved in the monoclinic $P2_1/c$ space group using XS²⁸ (incorporated in SHELXL). All non-hydrogen atoms were refined with anisotropic thermal parameters. All hydrogen atoms were placed in idealized positions and refined using a riding model. The structure was refined (weighted least-squares refinement on F^2) and the final least-squares refinement converged. No additional symmetry was found using ADDSYM incorporated in the PLATON program.²⁹

■ ASSOCIATED CONTENT

■ Supporting Information

The Supporting Information is available free of charge on the ACS Publications website at DOI: 10.1021/acs.organomet.6b00762.

NMR spectra (PDF)

crystallographic information (CIF)

■ AUTHOR INFORMATION

Corresponding Author

*E-mail for O.V.O.: ozerov@chem.tamu.edu.

ORCID

Oleg V. Ozerov: 0000-0002-5627-1120

Notes

The authors declare no competing financial interest.

■ ACKNOWLEDGMENTS

We are grateful to the National Science Foundation (grant CHE-1300299 to O.V.O.), the Welch Foundation (grant A-1717 to O.V.O.), and the Taiwan Ministry of Education (Graduate Fellowship for Study Abroad to W.-C.S.) for support of this research. We are grateful to Haomiao Xie for assistance with acquisition of IR spectra.

■ REFERENCES

- (1) (a) Gunanathan, C.; Milstein, D. *Chem. Rev.* **2014**, *114*, 12024–12087. (b) Selander, N.; Szabó, K. J. *Chem. Rev.* **2011**, *111*, 2048–2076. (c) Gunanathan, C.; Milstein, D. *Acc. Chem. Res.* **2011**, *44*, 588–602. (d) van der Boom, M. E.; Milstein, D. *Chem. Rev.* **2003**, *103*, 1759–1792.
- (2) (a) Gupta, M.; Hagen, C.; Flesher, R. J.; Kaska, W. C.; Jensen, C. M. *Chem. Commun.* **1996**, 2083–2084. (b) Gupta, M.; Hagen, C.; Kaska, W. C.; Cramer, R. E.; Jensen, C. M. *J. Am. Chem. Soc.* **1997**, *119*, 840–841. (c) Xu, W.; Rosini, G. P.; Krogh-Jespersen, K.; Goldman, A. S.; Gupta, M.; Jensen, C. M.; Kaska, W. C. *Chem. Commun.* **1997**, 2273–2274. (d) Liu, F.; Goldman, A. S. *Chem. Commun.* **1999**, 655–656. (e) Renkema, K. B.; Kissin, Y. V.; Goldman, A. S. *J. Am. Chem. Soc.* **2003**, *125*, 7770–7771. (f) Göttker-Schnetmann, I.; White, P.; Brookhart, M. *J. Am. Chem. Soc.* **2004**, *126*, 1804–1811. (g) Göttker-Schnetmann, I.; Brookhart, M. *J. Am. Chem. Soc.* **2004**, *126*, 9330–9338.
- (3) Choi, J.; MacArthur, A. H. R.; Brookhart, M.; Goldman, A. S. *Chem. Rev.* **2011**, *111*, 1761–1779.
- (4) (a) Yao, W.; Zhang, Y.; Jia, X.; Huang, Z. *Angew. Chem., Int. Ed.* **2014**, *53*, 1390–1394. (b) Nawara-Hultsch, A.; Hackenberg, J.; Punji, B.; Supplee, C.; Emge, T.; Bailey, B.; Schrock, R. R.; Brookhart, M.; Goldman, A. S. *ACS Catal.* **2013**, *3*, 2505–2514.
- (5) Segawa, Y.; Yamashita, M.; Nozaki, K. *J. Am. Chem. Soc.* **2009**, *131*, 9201–9203.
- (6) (a) Spokoyny, A. M.; Reuter, M. G.; Stern, C. L.; Ratner, M. A.; Seideman, T.; Mirkin, C. A. *J. Am. Chem. Soc.* **2009**, *131*, 9482–9483. (b) El-Zaria, M. E.; Arii, H.; Nakamura, H. *Inorg. Chem.* **2011**, *50*, 4149–4161. (c) Eleazer, B. J.; Smith, M. D.; Popov, A. A.; Peryshkov, D. V. *J. Am. Chem. Soc.* **2016**, *138*, 10531–10538.
- (7) (a) Tanoue, K.; Yamashita, M. *Organometallics* **2015**, *34*, 4011–4017. (b) Kwan, E. H.; Kawai, Y. J.; Kamakura, S.; Yamashita, M. *Dalton Trans.* **2016**, 45, 15931–15941.
- (8) (a) Lin, T.-P.; Peters, J. C. *J. Am. Chem. Soc.* **2014**, *136*, 13672–13683. (b) Hill, A. F.; McQueen, C. M. A. *Organometallics* **2014**, *33*, 1977–1985.
- (9) Shih, W.-C.; Gu, W.; MacInnis, M. C.; Timpa, S. D.; Bhuvanesh, N.; Zhou, J.; Ozerov, O. V. *J. Am. Chem. Soc.* **2016**, *138*, 2086–2089.
- (10) Bontemps, S.; Gornitzka, H.; Bouhadir, G.; Miqueu, K.; Bourissou, D. *Angew. Chem., Int. Ed.* **2006**, *45*, 1611–1614.
- (11) Schuhknecht, D.; Ritter, F.; Tauchert, M. E. *Chem. Commun.* **2016**, 52, 11823–11826.
- (12) On the basis of the procedure used for the synthesis of (PCP)IrH₄: (a) Gupta, M.; Hagen, C.; Flesher, R. J.; Kaska, W. C.; Jensen, C. M. *Chem. Commun.* **1996**, 2083–2084. (b) Gupta, M.; Hagen, C.; Kaska, W. C.; Cramer, R. E.; Jensen, C. M. *J. Am. Chem. Soc.* **1997**, *119*, 840–841.
- (13) Arnold, N.; Mozo, S.; Paul, U.; Radius, U.; Braunschweig, H. *Organometallics* **2015**, *34*, 5709–5715.
- (14) (a) Gloaguen, Y.; Bénac-Lestrille, G.; Vendier, L.; Helmstedt, U.; Clot, E.; Alcaraz, G.; Sabo-Etienne, S. *Organometallics* **2013**, *32*, 4868–4877. (b) Montiel-Palma, V.; Lumbierres, M.; Donnadiou, B.; Sabo-Etienne, S.; Chaudret, B. *J. Am. Chem. Soc.* **2002**, *124*, 5624–5625. (c) Lachaize, S.; Essalah, K.; Montiel-Palma, V.; Vendier, L.; Chaudret, B.; Barthelat, J.-C.; Sabo-Etienne, S. *Organometallics* **2005**, *24*, 2935–2943.
- (15) For X = BH₄, the BH₄ ligand is clearly type A.
- (16) Miyada, T.; Huang Kwan, E.; Yamashita, M. *Organometallics* **2014**, *33*, 6760–6770.
- (17) Wang, D. Y.; Choliy, Y.; Haibach, M. C.; Hartwig, J. F.; Krogh-Jespersen, K.; Goldman, A. S. *J. Am. Chem. Soc.* **2016**, *138*, 149–163.
- (18) (a) Hill, A. F. *Organometallics* **2006**, *25*, 4741–4743. (b) Parkin, G. *Organometallics* **2006**, *25*, 4744–4747.
- (19) Sircoglou, M.; Bontemps, S.; Bouhadir, G.; Saffon, N.; Miqueu, K.; Gu, W.; Mercy, M.; Chen, C.-H.; Foxman, B. M.; Maron, L.; Ozerov, O. V.; Bourissou, D. *J. Am. Chem. Soc.* **2008**, *130*, 16729–16738.
- (20) (a) Amgoune, A.; Bourissou, D. *Chem. Commun.* **2011**, 47 (3), 859–871. (b) Bouhadir, G.; Bourissou, D. *Chem. Soc. Rev.* **2016**, *45* (4), 1065–1079.
- (21) Anderson, J. S.; Rittle, J.; Peters, J. C. *Nature* **2013**, *501*, 84–87.
- (22) Addison, A. W.; Rao, T. N.; Reedijk, J.; van Rijn, J.; Verschoor, G. C. *J. Chem. Soc., Dalton Trans.* **1984**, 1349–1356.
- (23) Bézier, D.; Brookhart, M. *ACS Catal.* **2014**, *4*, 3411–3420.
- (24) Smith, J. D.; Logan, J. R.; Doyle, L. E.; Burford, R. J.; Sugawara, S.; Ohnita, C.; Yamamoto, Y.; Piers, W. E.; Spasyuk, D. M.; Borau-Garcia, J. *Dalton Trans.* **2016**, 45, 12669–12679.
- (25) Isomerization of 1-hexene into 2-hexene and 3-hexene was also observed.
- (26) APEX2, Version 2 User Manual, M86-E01078, Bruker Analytical X-ray Systems: Madison, WI, June 2006.
- (27) Sheldrick, G. M. SADABS (version 2008/1): Program for Absorption Correction for Data from Area Detector Frames; University of Göttingen, Göttingen, Germany, 2008.
- (28) Sheldrick, G. M. *Acta Crystallogr., Sect. A: Found. Crystallogr.* **2008**, *64*, 112–122.
- (29) Spek, A. L. *J. Appl. Crystallogr.* **2003**, *36*, 7–13.